Hindawi
Modelling and Simulation in Engineering
Volume 2024, Article ID 7931501, 12 pages
https://doi.org/10.1155/2024/7931501

Review Article

State of the Art of Modelling and Design Approaches for Ejectors in Proton Exchange Membrane Fuel Cell

Christian Antetomaso [1,2]

[1]*CNR STEMS, Naples, Italy*
[2]*University of Naples "Parthenope", Naples, Italy*

Correspondence should be addressed to Christian Antetomaso; christian.antetomaso@stems.cnr.it

Received 3 October 2023; Revised 17 January 2024; Accepted 18 March 2024; Published 5 April 2024

Academic Editor: Vijayanandh Raja

Proton exchange membrane fuel cell (PEMFC) has a promising future in the power generation and transportation fields. Recirculation of unused anodic gases is fundamental to achieve a high-performance energy system, and this is usually attained employing ejectors or pumps. With respect to the latter, ejectors present no moving parts, thus resulting in both higher overall efficiency of the system and lower maintenance cost. Their main drawback is represented by the narrow optimal operative range: the entrainment ratio (ER) greatly depends on primary pressure, working pressure, and operative condition in general. In the last decade, numerous authors focused their efforts on fully comprehending and correctly simulating their working principles and analyzing how geometrical parameters influence ER and design different geometries to enlarge the operative range. The aim of this paper is to present in an ordered and clear manner the state of the art of ejector design, both from simulative (turbulence model, single or multiphase stream, etc.) and empirical (commonly used "rule of thumb") points of view.

1. Introduction

PEMFC has been proven to be a possible solution for a green future in both transportation [1] and static power production [2]. It is a common practice to supply reaction gas with excess stoichiometric ratio to ensure high performance [3] of the cell and purge forming water droplets and impurities [4, 5]; thus, several researchers focused their effort on investigating various gas management strategies, with the predominant ideas being dead-end anode [6, 7] and excessive gas recirculation [8, 9]. In operating with a dead-end configuration, the cell presents good performance and high hydrogen utilization rate; however, employing this strategy for a prolonged period led to accumulation of inert gas and water, hence degrading cell over time. On the other hand, anodic gas recirculation system (ARS) requires the design, installation, and maintenance of an additional component, being it a pump or an ejector. Pumps have a wide operating range and relatively easy control but will increase power consumption and overall complexity of the system [10, 11]. Ejectors present themselves as an interesting option to play that role, given their advantages with respect to pumps: lower installation and maintenance cost, no moving parts, and no noise [12, 13].

Figure 1 shows a simplified scheme for an ARS that employs an ejector. The hydrogen is primarily supplied to the PEMFC from the high-pressure hydrogen tank; the gas travels through the serpentine, and then, the exceeding part is recovered in a secondary circuit. It is worth noting that the nature of this "recovered" flow, two-phase multispecies, poses one of the major issues with ejector simulation [14].

The ejector is essentially a device that uses the high pressure of a fluid to pump a low-pressure one.

Figure 2 shows the geometry of a simple ejector. The motive or primary fluid is the one at high pressure (P_p), while the secondary fluid resides at low pressure (P_s) are in a toroidal space. The motive fluid is initially accelerated through a nozzle (N_α, N_D) and thus creates a low-pressure region nearby its exit; this region is often referred to as

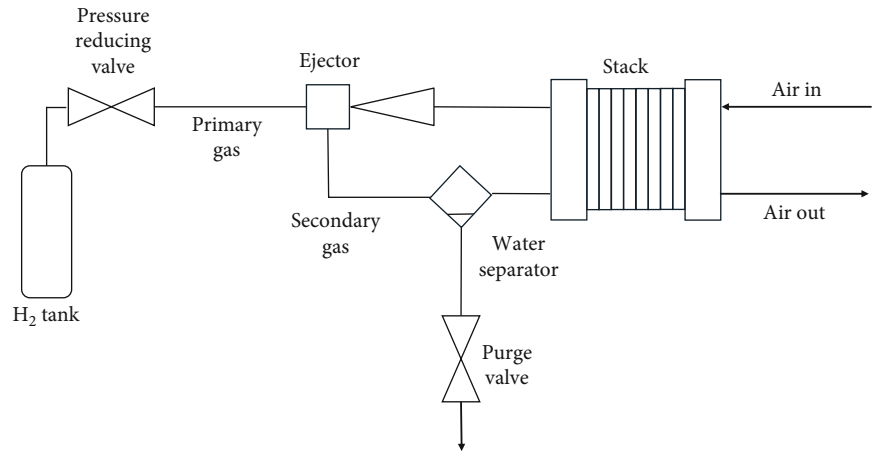

Figure 1: Scheme of simplified ARS.

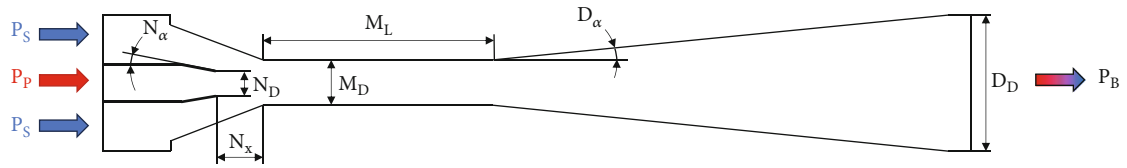

Figure 2: Geometrical scheme of an ejector.

suction chamber since the low-pressure fluid tends to move towards the motive fluid due to the pressure gradient. At this point, fluids start to mix in the mixing chamber (M_L, M_D) and finally expand in the divergent section (D_α, D_D) to recover kinetic energy and reach the required working pressure. An experimental schlieren visualization of this process is presented by Rao and Jagadeesh [15]. All the parameters shown in Figure 2 (and even more if we consider different geometries, e.g., convergent-divergent nozzle and multistage ejector) are fundamental during the design process, since they play an important role in determining the ER provided by the ejector, its optimal operative range, and critical condition. The ER is evaluated through the following formula:

$$\mathrm{ER} = \frac{\dot{m}_\mathrm{s}}{\dot{m}_\mathrm{p}}, \tag{1}$$

where $\dot{m}_\mathrm{s}$ and $\dot{m}_\mathrm{p}$ are the primary and secondary mass flow, respectively. Another important parameter to characterize ejectors is the range coefficient (R_{EJE}); it indicates the percentage of working condition that the designed ejector can cover with respect to the whole operative range of the system. In PEMFC system, it is usually in the range 65-80% [16]. It is calculated as follows:

$$R_\mathrm{EJE} = \frac{P_\mathrm{max} - P_\mathrm{min}}{P_\mathrm{peak}}, \tag{2}$$

where P_max and P_min are the maximum and minimum operating power and P_{peak} is the power peak of the fuel cell stack.

Figure 3 is useful to better understand how ER changes in the working range of the ejector. At fixed P_p and P_s, it is stable on its maximum value as P_B increases since both flows are chocked. This is the range for which the ejector was originally designed. As the backpressure surpasses a certain threshold, only the motive fluid is chocked, and the ER sharply decreases. If the backpressure continues to rise even further from the design point, reverse flow mode is reached. This means that the useful operative range of an ejector is quite narrow. Several authors investigated through experimental and simulative studies the effects of geometrical parameters, some even proposed novel ejector concepts (multinozzle, variable area, and so on). Deciding which model and thus which rule follow in designing an ejector for a specific purpose is quite tortuous due to the abundance of empiric rules that are presented in the literature. In this paper, the state of the art from both experimental and simulation point of view is presented and commented with the aim to provide an overlook on the most commonly used models.

2. Ejector Simulation

Due to the reciprocal influences of the various geometrical parameters of an ejector, the optimization of its design could be a long and expensive process. Proper modelling could be an invaluable tool to optimize this device and bring down prototyping costs. The first distinction that has to be made when talking about ejector modelling is whether to consider a constant pressure mixing (CPM) or constant area mixing (CAM) device. The substantial difference lays on the geometry of the designed suction chamber. Figure 4 visualizes

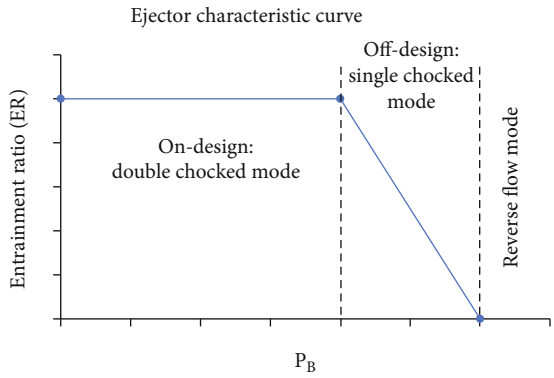

Figure 3: Ejector characteristic curve.

these design concepts. Their models were early developed by Keenan et al. [17] and still today represent the basis for ejector analysis and performance evaluation. CPM ejectors are considered more favourable for most applications since, even though they provide lower mass flow rate, they have the advantages of operating in a wider range of backpressures, thus showing higher working stability [18, 19]. At present, the two most adopted modelling approaches are the lumped parameter model (LPM) and computational fluid dynamics (CFD) model. The former is faster, but its prediction capability strongly depends on the parameter choice and how those are able to summarize local phenomena. On the other hand, CFD approach is far more time-consuming, and it has not a defined methodology. Historically speaking, density-based (DB) solver was used for its high-speed compressible flow [20], but it requires attention in imposing Courant-Friedrichs-Lewy (CFL) condition [21]. However, Van Vu and Kracik [22] compared DB and pressure-based (PB) solvers with a real gas model, evaluating a 1% discrepancy for ER, but also observing that PB resulted less time-consuming and more stable. Even more troubling is the simulation of turbulence inside this device. Reynolds-averaged Navier-Stokes (RANS) approach is generally used, but studies presented from different authors show contradictory results over which turbulence model should be adopted: even though global parameter (e.g., ER) can be similarly predicted with different turbulence model, the local flow phenomena may differ [23]. Mazzelli et al. [24] conducted numerical analysis using 4 different turbulence models (k–ε, k–ε realizable, k–ω SST, and the stress–ω Reynolds Stress), noticing that the best solution varies with the operative condition. In particular "ε models" are more accurate with low primary pressure, whereas k–ω SST showed the best overall performance. Besagni and Inzoli [25] confirmed that k–ω SST performs better than other models, showing good agreement in both global and local parameters. However, in the case of fuel cell ejector, Chen et al. [26] concluded that k–ε model is more accurate for low and medium flow rate, while k–ε realizable shows better agreement with experimental results at large flow rate. Xiao et al. [27] performed a comparative study varying solver, turbulence model, near-wall treatment, and spatial discretization scheme. They concluded that the results from PB solver are slightly closer to the experimental data with respect to the ones from DB. The standard k–ε model resulted very sensitive to the near-wall treatment; thus, the k–ω SST and the k–ε realizable (with standard wall function or enhanced wall treatment) are recommended. A different concern in simulating these devices lays on whether to consider a 2D axisymmetric or 3D domain. Both Pianthong et al. [28] and Gagan et al. [29] compared a 2D and 3D ejector model, concluding that, even though the 3-dimensional approach led to better accuracy, the axisymmetric assumption had a marginal influence on the model prediction capabilities, since it just slightly influenced axial velocity and pressure in the divergent region. However, Mazzelli et al. [24] noted that this effect may lead to large errors when operating in the off-design zone. It is worth noting that, when considering rectangular ejector cross-section, using the 2D or 3D approach may cause big discrepancies [30, 31]. One last concern regards the nature of the recirculating fluid, since it presents water vapor and thus condensation may occur inside the component. A commonly made assumption neglects the effect of this state-shift phenomenon, or even neglects the presence of water vapor at all, considering a dry hydrogen flux due to the complexity of this multiphase problem. However, both Wang et al. [32] and Ariafar et al. [33] confirmed that the wet steam model is able to better capture flow patterns inside the ejector. Han et al. [14, 34] performed two-phase simulations to weigh the effect of liquid water on the ejector efficiency. In [14], results showed an increase in temperature (due to latent heat of vaporization), lower velocity, and higher pressure of the gas phase due to condensation, resulting in a lower entrainment performance and better agreement with experimental results. In [34], the authors took into account both the homogeneous and the heterogeneous condensation. The two crucial factors that seem to influence the most droplet size were residence time and subcooling degree. Condensation process led to a mean efficiency reduction of 1.42%. From the experimental point of view, some studies have been conducted to visualize flow morphology and droplet distribution [35–37]; however, these studies often offer only a qualitative analysis of the phenomenon due to both visualization difficulties and hydrogen safety hazard.

3. Literature Review

Defining the optimal nozzle geometry is a fundamental step since it affects both entrainment ratio and critical backpressure. Metin et al. [38] used ANSYS Fluent to model an ejector under the single-phase axisymmetric flow assumption, concluding that the ER of the ejector could be increased up to 6% varying the primary nozzle position. It is worth noting that they also observed a critical point where while increasing NXP, the ER starts decreasing. Chen et al. [39] proposed an annular mixing layer theory: the idea is that the primary and secondary flow mix in an annular layer that grows as flow moves towards the ejector axis. The developed model is in good agreement with the experimental data and confirmed that the optimal nozzle exit position depends on the expansion ratio, thus on the working condition. Poirier [40] performed an extensive experimental campaign to verify the effect of working condition on nozzle optimal position. In one of the analyzed cases, the critical entrainment

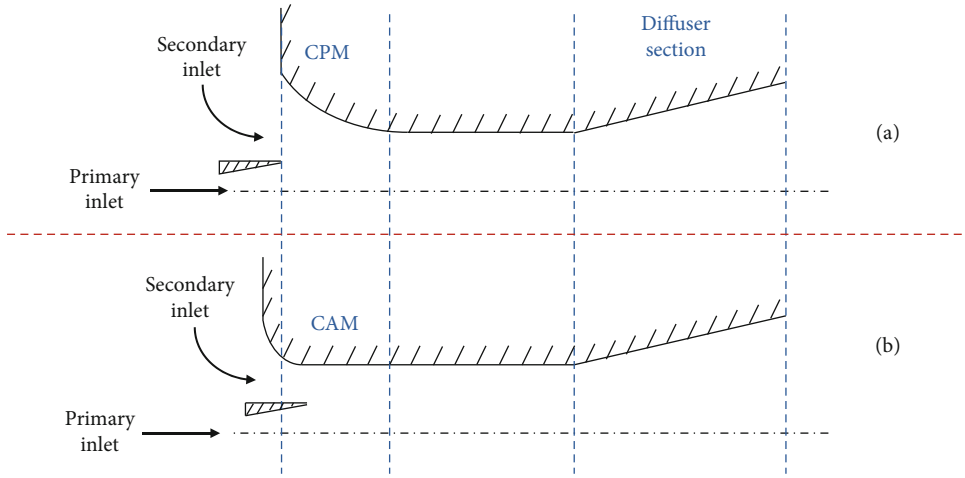

Figure 4: (a) CPM and (b) CAM (adapted from [18]).

ratio improved by 34% just by moving the nozzle. Moreover, he also observed multiple "optimal" N_X value, up to four peaks. Also, Rand et al. [41] experimentally and numerically investigated the presence of these suboptimal nozzle position points using the compound choking indicator: for a given operative point, this criterion highlights the location where the secondary flow is choked and allows to individuate the variation of choking position for several values of N_X. However, also the mixing chamber layout plays an important role in the ejector's overall performance. As a matter of fact, Pei et al. [42] proposed a CFD single-phase ideal gas model to perform a parametric study on the measures of interest of an ejector. In particular, they determined an optimal range for the ratio between mixing chamber and nozzle out diameter ($M_D/N_D = 3.00 - 3.54$) and between mixing chamber length and diameter ($M_L/M_D = 1 - 3$). Ma et al. [43] performed a 3D CFD simulation and, at set operative conditions, considered 4 geometrical parameters to be optimized with a user-defined priority: nozzle diameter, nozzle position, secondary inlet diameter, and mixing chamber diameter. It is clear by now that the design geometry strongly depends on the defined criterion; therefore, more complex and comprehensive optimization algorithms [44–50] are needed.

Table 1 reports a summary of the type of study performed, modelling adopted, and key findings for several literature papers.

4. Alternative Geometries

From the literature review presented in Table 1, it is clear that simulation and optimization led to an increase in ejector performance, but the narrow operational range issue still remains. Therefore, some researchers focused their efforts on investigating novel approach on ejector design: multistage, multinozzle, moving nozzle, nested nozzle, bypass circuit, and other solutions are hereby presented.

A simple solution is the introduction of a moving needle in the nozzle, allowing for operation with variable nozzle diameter and with the possibility to better control motive flow direction as it enters the suction chamber (see Figure 5). This solution needs a control strategy that properly set the correct nozzle effective area with respect to operative condition considered, but it is able to enlarge the range coefficient of the ejector [63–66]. However, the sealing, manufacturing costs, precise control, and long-time reliability are significant challenges.

Another conceptually simple solution is the usage of multiple ejectors [67–70], and the ad hoc control strategy realized by Chen et al. [71] for a 70 kW PEMFC using two identical ejectors was able to cover the stack's minimum 8% to maximum 100% power output.

Other authors investigated deeper change in ejector geometry. Chen et al. [72] observed a low-pressure zone in between mixing and diffuser section and proposed a motive fluid bypass to enlarge ER. The proposed solution (see Figure 6) showed good performance when compared to the original design: larger ER and lower critical backpressure.

Song et al. [73] simulated and experimentally investigated the performance of a twin-nozzle ejector, compared to the traditional one that improved the hydrogen recirculation under low load condition. The geometry proposed by Xue et al. [74] also employs a modified version of a nozzle which was divided into four small nozzles, as per Figure 7. The total mass flow rate passing through the novel nozzles is equal to the original one. In choosing the number, they had to consider the fact that, even though more nozzles lead to more flow rate step, it may also lead to malfunctioning in the single node operational mode. Simulation results confirmed that the multinozzle ejector expands the operating range by switching the working condition with different coactive nozzle strategies, thus effectively increasing the range coefficient. Another study [75] introduced a nested nozzle (see Figure 8), in which geometry was optimized through CFD in order to cover the whole operative range, from idle condition to full power. On a similar note, Du et al. [76] and Han et al. [77] investigated the performance of a coaxial nozzle, confirming the extension of operative range with respect to the default one. A different take on multistage ejectors is the one offered by Wang et al. [78]

Table 1: Literature survey on ejector simulation and geometric optimization.

Ref.	Year	Type	More details	Key findings
[38]	2019	Numerical	ANSYS Fluent, 2D axisymmetric steady flow, k–ω SST, 1-phase 1-species	Increasing N_X raises ER, after a certain value performance deteriorates
[39]	2020	Numerical	Thermodynamic model, annular mixing layer	Optimal N_X depends on working condition
[40]	2022	Experimental	Ejectors with different nozzle and area ratios tested over wide ranges of operating conditions	Up to 4 "optimal" N_X observed; these values were affected by both working condition and area ratios
[41]	2022	Mix	Experimental testing and validation of proposed model, ANSYS Fluent, 2D axisymmetric steady flow, k–ω SST, 1-phase 1-species, compound choking criterion	Compound choking allowed to determine variation in secondary flow choking position under several suboptimal N_X
[42]	2019	Numerical	ANSYS Fluent, 2D steady flow, k–ε; model coupled with anodic pressure drop formula, 1-phase 2-species	Optimal range for M_D/N_D (3.00–3.54) and M_L/M_D (1–3)
[43]	2021	Numerical	3D steady flow, RNG k–ε, 1-phase 2-species	N_D is the first geometrical parameter to be optimized
[51]	2014	Numerical	Thermodynamic model of ejector coupled with semiempirical stack model	Definition of two dimensionless parameters to guide ejector design
[52]	2017	Experimental	Ejector designed and tested at constant load and in fast transient condition	Anode gas recirculation rate ranging from 40% fuel utilization per pass at 25 A stack current to 64% fuel utilization per pass at 160 A stack current
[53]	2022	Numerical	ANSYS Fluent, 2D steady flow, k–ω SST, 1-phase 2-species	Determined order of influence of geometrical parameter: (i) Low current (110 A) $M_D > N_\alpha > N_L{}^* > N_X > M_L$ (ii) Middle current (275 A) $M_D > N_\alpha > N_L{}^* > M_L > N_X$ (iii) High current (412.5 A) $M_D > N_X > M_L > N_L{}^* > N_\alpha$ *Nozzle throat length
[54]	2013	Numerical	Thermodynamic model	Inlet primary flow temperature affects ejector entrainment ratio and component efficiency
[55]	2019	Mix	ANSYS Fluent, 2D axisymmetric steady flow, comparison between RNG k–ε and k–ω SST	RNG model shows higher accuracy than SST; optimal $D_\alpha = 11 - 13^\circ$ and $M_D = 5.9$ mm when stack works at its rated power
[56]	2020	Numerical	ANSYS Fluent, 2D axisymmetric steady flow, k–ω SST, coupled with a pressure drop through anode model	ER can be influenced by anode inlet temperature, relative humidity, and differential pressure
[57]	2020	Numerical	OpenFOAM, 3D transient flow, RNG $k-\varepsilon$, 2-phase 3-species	Dynamic responses during power variations results from velocity differences between the primary and the secondary flow; increase of nitrogen mass fraction promotes total ER, while it reduces hydrogen ER
[58]	2020	Numerical	COMSOL, 3D steady flow, coupled with MATLAB/Simulink hydrogen recovery system model	A lower ejector temperature is disadvantageous in removing the moisture content of the recirculated hydrogen gas, thus in practical applications; the hydrogen inlet temperature/pressure must be carefully controlled
[59]	2022	Numerical	Thermodynamic model of a 2-phase CPM ejector	ER increase from 0.47 to 1.14 as mixing area ratios range from 1.0 to 1.2 under the given conditions
[60]	2015	Numerical	Integrated lumped parameter-CFD approach, ANSYS Fluent, 2D axisymmetric steady flow, k–ω SST	The model can be used for studying off-design conditions, where ejector component efficiencies are not constant
[61]	2016	Numerical	ANSYS Fluent, 2D axisymmetric steady flow, RNG k–ε, 2-phase 1-species, optimization through genetic and evolutionary algorithm	M_D is the crucial parameter in ejector performance
[62]	2021	Numerical	ANSYS Fluent, 2D steady flow, RNG k–ε, 1-phase 2-species	Humidity and temperature of the secondary flow have a noticeable influence on the performance of the ejector
[44]	2017	Numerical	Thermodynamic model, hybrid fish swarm algorithm	Optimization efficiency increased with respect to genetic algorithm

Table 1: Continued.

Ref.	Year	Type	More details	Key findings
[45]	2018	Numerical	Multiobjective evolutionary algorithm coupled with a surrogate model based on CFD simulations	N_D and M_D are the most important geometrical variable; entrainment ratio can be increased up to 110% and 35%, for air and CO2, respectively
[46]	2023	Numerical	ANSYS Fluent, 2D axisymmetric steady flow, response surface methodology	Priority order in optimizing ejector geometry: $M_D > M_L > N_X$
[47]	2014	Numerical	2D axisymmetric steady flow, RNG k–ε, 1-phase 2-species, artificial neural network and genetic algorithm to obtain optimal geometry	Optimal $M_L/M_D = 6$; optimal $N_X = 0.52 \times M_D$; optimal $D_\alpha = 2.5 - 3^\circ$; optimal $D_D = 24 \times M_D$
[48]	2021	Numerical	Automated CFD workflow, ANSYS Fluent, RNG k–ε, 2-phase 1-species, Gaussian process regression machine learning model	The algorithm can be used to efficiently explore ejector designs with mean average errors between 0.07 and 0.1
[49]	2022	Numerical	ANSYS Fluent, 2D steady flow, realizable k–ε, optimization via adjoint method	ER increased by around 37%
[50]	2022	Numerical	MATLAB and experimental dataset of a steam-centered ejector are applied to train the ANN model of a steam ejector using three different algorithms	LM model yielded the best agreement; the effect of the outlet area ratio is less important with respect to throat area ratio

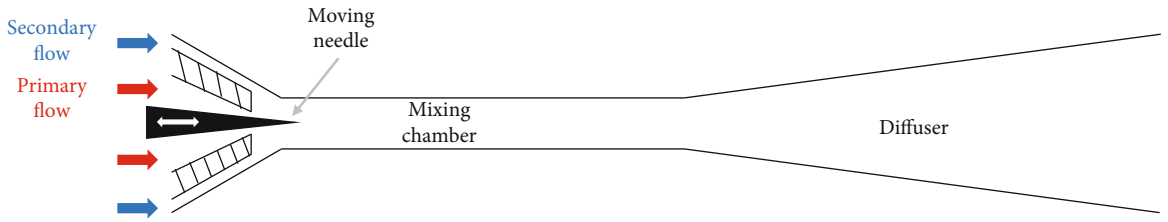

Figure 5: Scheme of variable geometry ejector (adapted from [63]).

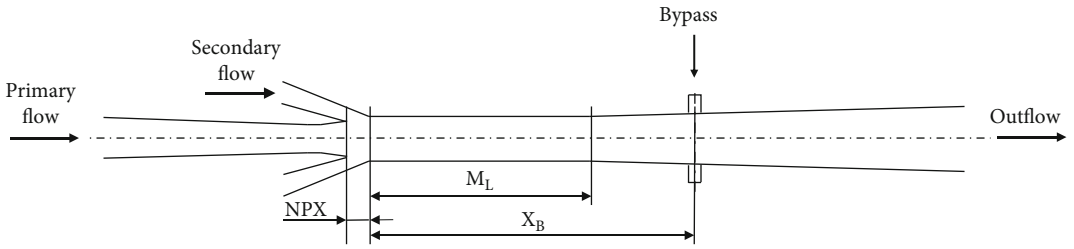

Figure 6: Scheme of ejector with bypass (adapted from [72]).

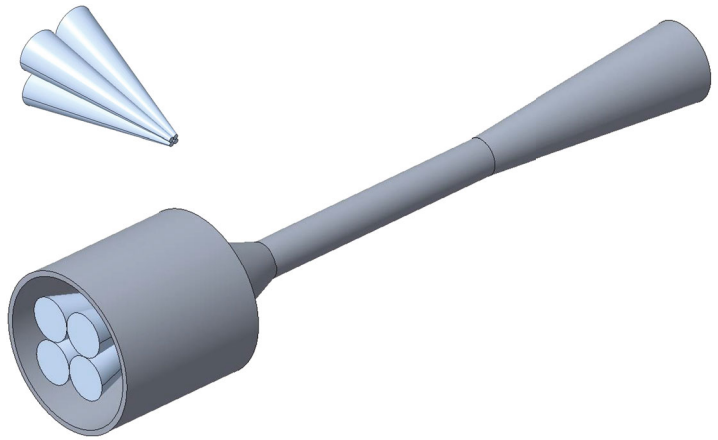

Figure 7: CAD of multinozzle layout (adapted from [74]).

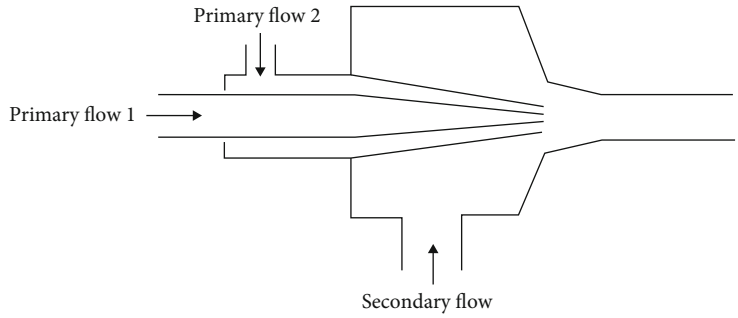

Figure 8: Schematic of nested nozzle concept (adapted from [76]).

and shown in Figure 9: it is a geometry not as compact as the one shown in Figure 8 but still offers an increase in ER of around 30%.

5. System Integration and Control

Other than the ejector itself, the whole PEMFC energy system must be considered when designing this component [16]. First, the anodic side usually requires the presence of a gas-water separator in order to remove most of the humidity from the recirculating circuit. The three mainly used separator types are presented in Figure 10. Even though cyclone and filter separator are characterized by a high-phase separation efficiency, they also cause larger pressure drop with respect to baffle one; regardless from the selected ARS, a lower recirculating pressure implies overall worst operative condition for the system. Han et al. [79] focused their efforts on optimizing a baffle separator through CFD simulations. In particular, three different structures were developed for a 75 kW PEMFC and analyzed both experimentally and numerically. For a comparable pressure drop, the optimum geometry ensures better separation efficiency.

On a different note, Ma et al. [80] designed a novel cyclone water separator system for a 40 kW PEMFC and investigated the flow field characteristics through CFD simulations. The new concept was designed with a volute inlet to boost the swirling effect, leading to enhanced centrifugal effect and steadier performance throughout the flow rate range. However, even in the presence of this component, a suitable purging phase has to be carefully chosen to fulfil two main functions: it removes inert gases that may accumulate in the anode due to membrane permeability and eliminates impure hydrogen [81]. Nitrogen may cross from cathode to anode through membrane due to the concentration gradient, and its accumulation negatively impacts the ER [62]. At the same time, a high purging frequency increases hydrogen consumption and leads to pressure fluctuations that may damage the membrane [82, 83]: keeping the pressure difference within the threshold with fast transient responses is a crucial issue for the safe operation of PEM fuel cell system [84]. For what regards ejector integration in the overall energy system, as shown in the previous chapter, different geometries have been proposed through years since the simple design suffers of low range coefficient. In [69], a comparative study was performed between single- and dual-ejector layouts, with the latter being able to cover the whole PEMFC-operating range. However, the authors noted that during the switching phase, pressure oscillations may undermine the lifetime of the membrane; thus, adequate control strategies are required. Thompson et al. [85] performed an analysis cost for an 80 kW light duty vehicle. They considered dual static ejectors (and relative control valves) for the ARS; nevertheless, they hinted to the fact that, according to their model, a single pulsed ejector may represent a valid solution: it shows the lower volume, lower power request, and lower production cost. Singer et al. [86] designed and performed numerical and experimental investigations on a pulsed injector-ejector unit. Ejectors are usually designed to work at full load, but the pulsed one is a very promising approach to cover the highly dynamic load of the automotive market. A solenoid valve just before the ejector nozzle can be opened for a desired period and frequency, ensuring proper stoichiometric value at anode inlet even at low load.

In this context, control strategies are of fundamental importance [87, 88]. As a matter of fact, the needle position in a variable area nozzle, the activation in a multiejector layout, and the opening in a multinozzle ejector all require an ad hoc control to cover low to medium system load. Qin et al. [89] proposed a classic PID to control the hydrogen mass flow by regulating a proportional valve just before the ejector body; the study reported a regulating time below 4.5 seconds under several load conditions. In [63], a variable geometry ejector is responsible for recirculating hydrogen in the cell, a stepper motor-leadscrew-based linear actuator control needle positioning, thus changing the effective nozzle diameter. Experiments suggested that the implemented PID algorithm produced considerable unnecessary motion of the needle. To overcome this issue, the derivative part of the controller was removed and a dead-band was added to the calculated pressure error. The new PI controller was able to provide the required hydrogen stoichiometry. Moreover, the ejector showed a good tolerance to liquid water, experiencing only momentary pressure drops. In [90], a common rail hydrogen injection+ejector system is implemented, and a Mamdani fuzzy controller is designed to regulate the hydrogen pressure. The controller evaluates the error between the hydrogen pressure setpoint and its actual value and also the error change rate, giving as output the change of the pulse width of the injection phase. Sankar

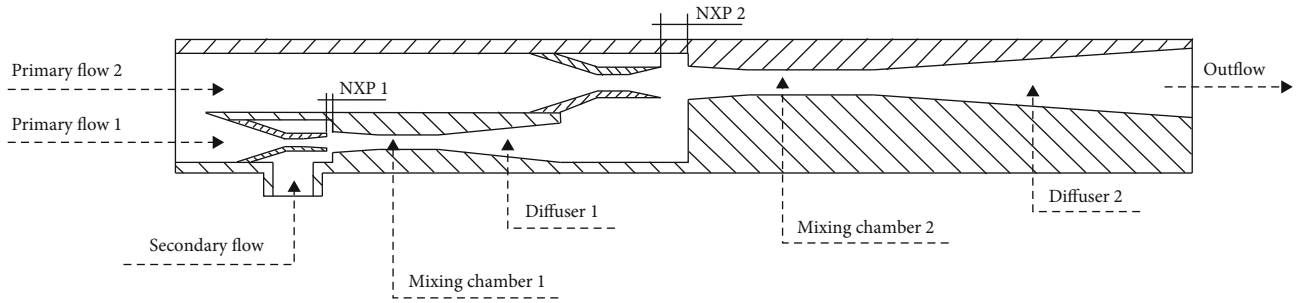

Figure 9: Scheme of a two-stage ejector (adapted from [78]).

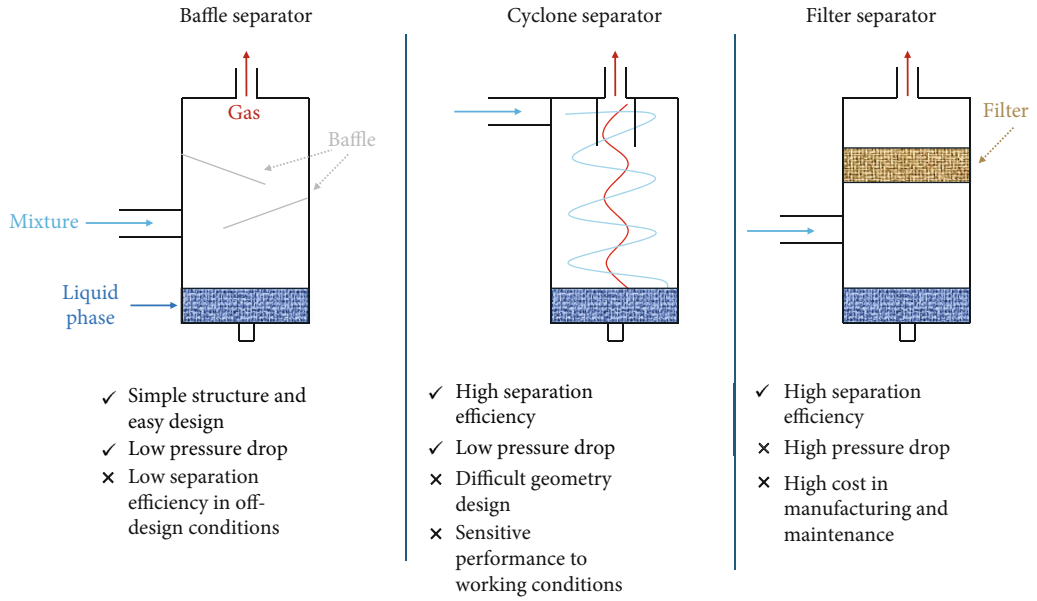

Figure 10: Schematic of the most common gas-liquid separator (adapted from [79]).

and Jana [91] proposed a multi-input multioutput (MIMO) sliding mode controller with the aim of maximizing membrane lifetime. Selected inputs were anode source pressure, compressor motor voltage, and cooling water flow; measured outputs were output cell voltage, compressor airflow, and system temperature. An adaptive supertwisting (ASTW) sliding mode algorithm is developed for the cooperative control of fuel and air feeding in PEMFC by Yin et al. [92]. Hydrogen excess ratio was aimed to a constant 1.5, while optimal oxygen excess ratio was taken from the literature table, given the current. It is worth noting that, since the air compressor has to dynamically adjust to the controller request, the membrane may suffer efficiency/useful life loss; thus, this value has to be monitored with caution. Reported results show an improved regulation time and smaller overshoot for an ASTW controller with respect to a conventional PID one.

6. Summary

Fuel cell systems can represent a step forward in the direction of cleaner and greener future, but the technology itself is still not mature. The design of an effective and efficient ARS could help its spread. In this work, a literature review on ejector modelling, geometry optimization, and possible alternative configurations is presented. The following conclusions can be drawn:

(i) There are lots of papers that investigate the optimization of ejector geometrical features with different modelling approaches (thermodynamic model, CFD 2D axisymmetric/3D, etc.) and different optimization rules (single-object, multiobject, adjoint method, etc.), but the reported results show sometimes contradictory findings. The reason of this inconsistency is due to the great influence that both working fluid and working conditions have on the optimal geometry. A robust workflow for ejector simulation is still to be developed. As a matter of fact, the chosen turbulence model influences the simulation behavior in the region near the jet core and there is no defined recommended model. Moreover, most of the reported literature focused their efforts on simulating the simple ejector geometry; thus, it is recommended to perform those simulations also for alternative geometries and/or different ARS layouts

(ii) Flow condensation phenomena inside the ejector are usually neglected, but some studies have been conducted both from experimental and numerical points of view; given the lack of a sturdy workflow, it is recommended to conduct numerical simulations of this two-phase flow varying the adopted turbulence model. This may give some insight on what could be the best way to simulate ejectors

(iii) Even though there are some differences in the adopted methodology, researchers seem to agree that the dimensionless ratios M_D/N_N and M_L/M_D, the nozzle diameter N_D, and its position N_X are the most important geometrical parameters in the ejector design. Some studies even reported the presence of multiple suboptimal nozzle position; thus, it is of focal importance to correctly chose this value

(iv) Some alternative geometries and control strategy are reported in the last part of the paper. It is worth noting that the simplicity of the ejector was one of its best "selling point"; however, its implementation in real working system requires some tweaks; the sealing and manufacturing cost for a variable ejector nozzle, or the proper control of pressure oscillation during switching phase for a twin ejector layout, are still significant challenges

Acronyms

ARS: Anodic gas recirculation system
ASTW: Adaptive supertwisting
CAM: Constant pressure mixing
CFD: Computational fluid dynamics
CFL: Courant-Friedrichs-Lewy
CPM: Constant area mixing
DB: Density based
ER: Entrainment ratio
LPM: Lumped parameter model
MIMO: Multi-input multioutput
PB: Pressure based
PEMFC: Proton exchange membrane fuel cell
RANS: Reynolds-averaged Navier-Stokes.

Symbols

P_p: Primary/motive pressure
P_s: Secondary pressure
P_B: Outlet pressure
N_α: Nozzle angle
N_D: Nozzle outlet diameter
N_X: Nozzle X position
M_L: Mixing chamber length
M_D: Mixing chamber diameter
D_α: Divergent angle
D_D: Divergent outlet diameter
$\dot{m}_s$: Secondary mass flow
$\dot{m}_p$: Primary mass flow.

Data Availability

The numeric results and experimental data presented in this review are from previously reported studies and datasets, which have been cited.

Conflicts of Interest

The author declares that he has no conflict of interests regarding the publication of this paper.

Acknowledgments

The author gratefully acknowledges the partial financial support of the European Union, NextGenerationEU—in the framework of the National Sustainable Mobility Center—MOST (CN00000023) and Italian Ministry of University and Research Decree no. 1033 (17/06/2022, Spoke 12).

References

[1] H. He, S. Quan, and Y. X. Wang, "Hydrogen circulation system model predictive control for polymer electrolyte membrane fuel cell-based electric vehicle application," *International Journal of Hydrogen Energy*, vol. 45, no. 39, pp. 20382–20390, 2020.

[2] O. Z. Sharaf and M. F. Orhan, "An overview of fuel cell technology: fundamentals and applications," *Renewable and Sustainable Energy Reviews*, vol. 32, pp. 810–853, 2014.

[3] T. V. Reshetenko, G. Bender, K. Bethune, and R. Rocheleau, "Systematic study of back pressure and anode stoichiometry effects on spatial PEMFC performance distribution," *Electrochimica Acta*, vol. 56, no. 24, pp. 8700–8710, 2011.

[4] C. Zhang, W. Zhou, L. Zhang, S. H. Chan, and Y. Wang, "An experimental study on anode water management in high temperature PEM fuel cell," *International Journal of Hydrogen Energy*, vol. 40, no. 13, pp. 4666–4672, 2015.

[5] M. Steinberger, J. Geiling, R. Oechsner, and L. Frey, "Anode recirculation and purge strategies for PEM fuel cell operation with diluted hydrogen feed gas," *Applied Energy*, vol. 232, pp. 572–582, 2018.

[6] S. Liu, T. Chen, C. Zhang, and Y. Xie, "Study on the performance of proton exchange membrane fuel cell (PEMFC) with dead-ended anode in gravity environment," *Applied Energy*, vol. 261, article 114454, 2020.

[7] J. C. Kurnia, A. P. Sasmito, and T. Shamim, "Advances in proton exchange membrane fuel cell with dead-end anode operation: a review," *Applied Energy*, vol. 252, article 113416, 2019.

[8] S. Rodosik, J. P. Poirot-Crouvezier, and Y. Bultel, "Impact of humidification by cathode exhaust gases recirculation on a PEMFC system for automotive applications," *International Journal of Hydrogen Energy*, vol. 44, no. 25, pp. 12802–12817, 2019.

[9] H. Y. Lee, H. C. Su, and Y. S. Chen, "A gas management strategy for anode recirculation in a proton exchange membrane fuel cell," *International Journal of Hydrogen Energy*, vol. 43, no. 7, pp. 3803–3808, 2018.

[10] Y. Liu, Z. Tu, and S. H. Chan, "Performance analysis and dynamic characteristics of a proton exchange membrane fuel cell with dual recirculation pumps for air-free applications," *Journal of Power Sources*, vol. 566, article 232926, 2023.

[11] H. J. Bae, H. S. Ban, Y. G. Noh et al., "The study of the design and control for the hydrogen recirculation blower noise and vibration reduction," *Transactions of the Korean Hydrogen and New Energy Society*, vol. 25, no. 5, pp. 509–515, 2014.

[12] Y. Liu, Z. Tu, and S. H. Chan, "Applications of ejectors in proton exchange membrane fuel cells: a review," *Fuel Processing Technology*, vol. 214, article 106683, 2021.

[13] B. M. Tashtoush, A. A. N. Moh'd, and M. A. Khasawneh, "A comprehensive review of ejector design, performance, and applications," *Applied Energy*, vol. 240, pp. 138–172, 2019.

[14] J. Han, J. Feng, and X. Peng, "Phase change characteristics and their effect on the performance of hydrogen recirculation ejectors for PEMFC systems," *International Journal of Hydrogen Energy*, vol. 47, no. 2, pp. 1144–1156, 2022.

[15] S. Rao and G. Jagadeesh, "Observations on the non-mixed length and unsteady shock motion in a two dimensional supersonic ejector," *Physics of Fluids*, vol. 26, no. 3, 2014.

[16] J. Han, J. Feng, P. Chen, Y. Liu, and X. Peng, "A review of key components of hydrogen recirculation subsystem for fuel cell vehicles," *Energy Conversion and Management: X*, vol. 15, article 100265, 2022.

[17] J. H. Keenan, E. P. Neumann, and F. Lustwerk, "An investigation of ejector design by analysis and experiment," *Journal of Applied Mechanics*, vol. 17, no. 3, pp. 299–309, 1950.

[18] D. W. Sun and I. W. Eames, "Recent developments in the design theories and applications of ejectors-a review," *Fuel and Energy Abstracts*, vol. 5, no. 36, p. 361, 1995.

[19] S. He, Y. Li, and R. Z. Wang, "Progress of mathematical modeling on ejectors," *Renewable and Sustainable Energy Reviews*, vol. 13, no. 8, pp. 1760–1780, 2009.

[20] T. Sriveerakul, S. Aphornratana, and K. Chunnanond, "Performance prediction of steam ejector using computational fluid dynamics: part 1. Validation of the CFD results," *International Journal of Thermal Sciences*, vol. 46, no. 8, pp. 812–822, 2007.

[21] J. G. Del Valle, J. Sierra-Pallares, P. G. Carrascal, and F. C. Ruiz, "An experimental and computational study of the flow pattern in a refrigerant ejector. Validation of turbulence models and real-gas effects," *Applied Thermal Engineering*, vol. 89, pp. 795–811, 2015.

[22] N. Van Vu and J. Kracik, "CFD simulation of ejector: is it worth to use real gas models?," *EPJ Web of Conferences*, vol. 180, article 02075, 2018.

[23] A. Hemidi, F. Henry, S. Leclaire, J. M. Seynhaeve, and Y. Bartosiewicz, "CFD analysis of a supersonic air ejector. Part II: relation between global operation and local flow features," *Applied Thermal Engineering*, vol. 29, no. 14-15, pp. 2990–2998, 2009.

[24] F. Mazzelli, A. B. Little, S. Garimella, and Y. Bartosiewicz, "Computational and experimental analysis of supersonic air ejector: turbulence modeling and assessment of 3D effects," *International Journal of Heat and Fluid Flow*, vol. 56, pp. 305–316, 2015.

[25] G. Besagni and F. Inzoli, "Computational fluid-dynamics modeling of supersonic ejectors: screening of turbulence modeling approaches," *Applied Thermal Engineering*, vol. 117, pp. 122–144, 2017.

[26] F. Chen, M. Hou, J. Li, Y. Pei, and Y. Wang, "Proton exchange membrane fuel cell ejector test platform design and ejector test analysis," *World Electric Vehicle Journal*, vol. 12, no. 3, p. 103, 2021.

[27] J. Xiao, Q. Wu, L. Chen et al., "Assessment of different CFD modeling and solving approaches for a supersonic steam ejector simulation," *Atmosphere*, vol. 13, no. 1, p. 144, 2022.

[28] K. Pianthong, W. Seehanam, M. Behnia, T. Sriveerakul, and S. Aphornratana, "Investigation and improvement of ejector refrigeration system using computational fluid dynamics technique," *Energy Conversion and Management*, vol. 48, no. 9, pp. 2556–2564, 2007.

[29] J. Gagan, K. Smierciew, D. Butrymowicz, and J. Karwacki, "Comparative study of turbulence models in application to gas ejectors," *International Journal of Thermal Sciences*, vol. 78, pp. 9–15, 2014.

[30] A. B. Little, Y. Bartosiewicz, and S. Garimella, "Visualization and validation of ejector flow field with computational and first-principles analysis," *Journal of Fluids Engineering*, vol. 137, no. 5, article 051107, 2015.

[31] K. M. Arun, S. Tiwari, and A. Mani, "Three-dimensional numerical investigations on rectangular cross-section ejector," *International Journal of Thermal Sciences*, vol. 122, pp. 257–265, 2017.

[32] X. D. Wang, H. J. Lei, J. L. Dong, and J. Y. Tu, "The spontaneously condensing phenomena in a steam-jet pump and its influence on the numerical simulation accuracy," *International Journal of Heat and Mass Transfer*, vol. 55, no. 17-18, pp. 4682–4687, 2012.

[33] K. Ariafar, D. Buttsworth, G. Al-Doori, and R. Malpress, "Effect of mixing on the performance of wet steam ejectors," *Energy*, vol. 93, pp. 2030–2041, 2015.

[34] J. Han, Y. Chen, J. Feng, Z. Pang, and X. Peng, "Condensation and droplet characteristics in hydrogen recirculation ejectors for PEM fuel cell systems," *International Journal of Heat and Mass Transfer*, vol. 222, article 125098, 2024.

[35] M. Palacz, J. Bodys, M. Haida, J. Smolka, and A. J. Nowak, "Two-phase flow visualisation in the R744 vapour ejector for refrigeration systems," *Applied Thermal Engineering*, vol. 210, article 118322, 2022.

[36] A. B. Little and S. Garimella, "Shadowgraph visualization of condensing R134a flow through ejectors," *International Journal of Refrigeration*, vol. 68, pp. 118–129, 2016.

[37] A. Bouhanguel, P. Desevaux, and E. Gavignet, "Flow visualization in supersonic ejectors using laser tomography techniques," *International Journal of Refrigeration*, vol. 34, no. 7, pp. 1633–1640, 2011.

[38] C. Metin, O. Gök, A. U. Atmaca, and A. Erek, "Numerical investigation of the flow structures inside mixing section of the ejector," *Energy*, vol. 166, pp. 1216–1228, 2019.

[39] H. Chen, J. Zhu, J. Ge, W. Lu, and L. Zheng, "A cylindrical mixing chamber ejector analysis model to predict the optimal nozzle exit position," *Energy*, vol. 208, article 118302, 2020.

[40] M. Poirier, "Influence of operating conditions on the optimal nozzle exit position for vapor ejector," *Applied Thermal Engineering*, vol. 210, article 118377, 2022.

[41] C. P. Rand, S. Croquer, M. Poirier, and S. Poncet, "Optimal nozzle exit position for a single-phase ejector (experimental, numerical and thermodynamic modelling)," *International Journal of Refrigeration*, vol. 144, pp. 108–117, 2022.

[42] P. Pei, P. Ren, Y. Li et al., "Numerical studies on wide-operating-range ejector based on anodic pressure drop characteristics in proton exchange membrane fuel cell system," *Applied Energy*, vol. 235, pp. 729–738, 2019.

[43] T. Ma, M. Cong, Y. Meng, K. Wang, D. Zhu, and Y. Yang, "Numerical studies on ejector in proton exchange membrane fuel cell system with anodic gas state parameters as design boundary," *International Journal of Hydrogen Energy*, vol. 46, no. 78, pp. 38841–38853, 2021.

[44] S. Bai, L. Wang, and X. Wang, "Optimization of ejector geometric parameters with hybrid artificial fish swarm algorithm for PEM fuel cell," in *2017 Chinese Automation Congress (CAC)*, pp. 3319–3322, Jinan, China, 2017.

[45] J. A. E. Carrillo, F. J. S. de La Flor, and J. M. S. Lissén, "Single-phase ejector geometry optimisation by means of a multi-objective evolutionary algorithm and a surrogate CFD model," *Energy*, vol. 164, pp. 46–64, 2018.

[46] W. Song, X. Shen, Y. Huang, P. Jiang, and Y. Zhu, "Fuel ejector design and optimization for solid oxide fuel cells using response surface methodology and multi-objective genetic algorithm," *Applied Thermal Engineering*, vol. 232, article 121067, 2023.

[47] A. Maghsoodi, E. Afshari, and H. Ahmadikia, "Optimization of geometric parameters for design a high-performance ejector in the proton exchange membrane fuel cell system using artificial neural network and genetic algorithm," *Applied Thermal Engineering*, vol. 71, no. 1, pp. 410–418, 2014.

[48] K. E. Ringstad, K. Banasiak, Å. Ervik, and A. Hafner, "Machine learning and CFD for mapping and optimization of CO_2 ejectors," *Applied Thermal Engineering*, vol. 199, article 117604, 2021.

[49] H. Samsam-Khayani, S. H. Park, M. Y. Ha, K. C. Kim, and S. Y. Yoon, "Design modification of two-dimensional supersonic ejector via the adjoint method," *Applied Thermal Engineering*, vol. 200, article 117674, 2022.

[50] K. Zhang, Z. Zhang, Y. Han, Y. Gu, Q. Qiu, and X. Zhu, "Artificial neural network modeling for steam ejector design," *Applied Thermal Engineering*, vol. 204, article 117939, 2022.

[51] M. Dadvar and E. Afshari, "Analysis of design parameters in anodic recirculation system based on ejector technology for PEM fuel cells: a new approach in designing," *International Journal of Hydrogen Energy*, vol. 39, no. 23, pp. 12061–12073, 2014.

[52] K. Nikiforow, P. Koski, and J. Ihonen, "Discrete ejector control solution design, characterization, and verification in a 5 kW PEMFC system," *International Journal of Hydrogen Energy*, vol. 42, no. 26, pp. 16760–16772, 2017.

[53] C. Li, B. Sun, and Q. Luo, "Effect of structural parameters and operational characteristic analysis on ejector used in proton exchange membrane fuel cell," *Sustainability*, vol. 14, no. 15, p. 9205, 2022.

[54] V. Liso, N. M. Pagh, and K. S. Knudsen, "Ejector design and performance evaluation for recirculation of anode gas in a micro combined heat and power systems based on solid oxide fuel cell," *Applied Thermal Engineering*, vol. 54, no. 1, pp. 26–34, 2013.

[55] X. Wang, S. Xu, and C. Xing, "Numerical and experimental investigation on an ejector designed for an 80 kW polymer electrolyte membrane fuel cell stack," *Journal of Power Sources*, vol. 415, pp. 25–32, 2019.

[56] Y. Yang, W. Du, T. Ma et al., "Numerical studies on ejector structure optimization and performance prediction based on a novel pressure drop model for proton exchange membrane fuel cell anode," *International Journal of Hydrogen Energy*, vol. 45, no. 43, pp. 23343–23352, 2020.

[57] Z. Liu, Z. Liu, K. Jiao, Z. Yang, X. Zhou, and Q. Du, "Numerical investigation of ejector transient characteristics for a 130-kW PEMFC system," *International Journal of Energy Research*, vol. 44, no. 5, pp. 3697–3710, 2020.

[58] J. K. Kuo, W. Z. Jiang, C. H. Li, and T. H. Hsu, "Numerical investigation into hydrogen supply stability and I-V performance of PEM fuel cell system with passive Venturi ejector," *Applied Thermal Engineering*, vol. 169, article 114908, 2020.

[59] Y. Liu, M. Yu, and J. Yu, "An improved 1-D thermodynamic modeling of small two-phase ejector for performance prediction and design," *Applied Thermal Engineering*, vol. 204, article 118006, 2022.

[60] G. Besagni, R. Mereu, P. Chiesa, and F. Inzoli, "An integrated lumped parameter-CFD approach for off-design ejector performance evaluation," *Energy Conversion and Management*, vol. 105, pp. 697–715, 2015.

[61] M. Palacz, J. Smolka, W. Kus et al., "CFD-based shape optimisation of a CO_2 two-phase ejector mixing section," *Applied Thermal Engineering*, vol. 95, pp. 62–69, 2016.

[62] Z. Hailun, W. Sun, H. Xue, W. Sun, L. Wang, and L. Jia, "Performance analysis and prediction of ejector based hydrogen recycle system under variable proton exchange membrane fuel cell working conditions," *Applied Thermal Engineering*, vol. 197, article 117302, 2021.

[63] D. A. Brunner, S. Marcks, M. Bajpai, A. K. Prasad, and S. G. Advani, "Design and characterization of an electronically controlled variable flow rate ejector for fuel cell applications," *International Journal of Hydrogen Energy*, vol. 37, no. 5, pp. 4457–4466, 2012.

[64] D. Jenssen, O. Berger, and U. Krewer, "Improved PEM fuel cell system operation with cascaded stack and ejector-based recirculation," *Applied Energy*, vol. 195, pp. 324–333, 2017.

[65] F. Liu, H. Liu, Y. Liu et al., "Transient numerical study of CO_2 two-phase flow in a needle adjustable ejector," *International Journal of Heat and Mass Transfer*, vol. 214, article 124395, 2023.

[66] S. Baba, S. Takahashi, N. Kobayashi, and S. Hirano, "Performance of anodic recirculation by a variable flow ejector for a solid oxide fuel cell system under partial loads," *International Journal of Hydrogen Energy*, vol. 45, no. 16, pp. 10039–10049, 2020.

[67] M. Kim, W. Y. Lee, and C. S. Kim, "Development of the variable multi-ejector for a mini-bus PEMFC system," *ECS Transactions*, vol. 5, no. 1, pp. 773–780, 2007.

[68] E. Hosseinzadeh, M. Rokni, M. Jabbari, and H. Mortensen, "Numerical analysis of transport phenomena for designing of ejector in PEM forklift system," *International Journal of Hydrogen Energy*, vol. 39, no. 12, pp. 6664–6674, 2014.

[69] D. T. Le Tri, H. N. Vu, H. L. Nguyen, Y. Kim, and S. Yu, "A comparative study of single and dual ejector concepts for anodic recirculation system in high-performance vehicular proton exchange membrane fuel cells," *International Journal of Hydrogen Energy*, vol. 48, no. 70, pp. 27344–27360, 2023.

[70] P. Gullo, A. Hafner, K. Banasiak, S. Minetto, and E. E. Kriezi, "Multi-ejector concept: a comprehensive review on its latest technological developments," *Energies*, vol. 12, no. 3, p. 406, 2019.

[71] L. Chen, K. Xu, Z. Yang, Z. Yan, and Z. Dong, "Optimal design and operation of dual-ejector PEMFC hydrogen supply and circulation system," *Energies*, vol. 15, no. 15, p. 5427, 2022.

[72] W. Chen, H. Chen, C. Shi, K. Xue, D. Chong, and J. Yan, "A novel ejector with a bypass to enhance the performance," *Applied Thermal Engineering*, vol. 93, pp. 939–946, 2016.

[73] Y. Song, X. Wang, L. Wang, F. Pan, W. Chen, and F. Xi, "A twin-nozzle ejector for hydrogen recirculation in wide power operation of polymer electrolyte membrane fuel cell system," *Applied Energy*, vol. 300, article 117442, 2021.

[74] H. Xue, L. Wang, H. Zhang, L. Jia, and J. Ren, "Design and investigation of multi-nozzle ejector for PEMFC hydrogen recirculation," *International Journal of Hydrogen Energy*, vol. 45, no. 28, pp. 14500–14516, 2020.

[75] L. Chen, K. Xu, Z. Yang, Z. Yan, C. Zhai, and Z. Dong, "Optimal design of a novel nested-nozzle ejector for PEMFC's hydrogen supply and recirculation system," *International Journal of Hydrogen Energy.*, vol. 48, no. 70, pp. 27330–27343, 2023.

[76] Z. Du, Q. Liu, X. Wang, and L. Wang, "Performance investigation on a coaxial-nozzle ejector for PEMFC hydrogen recirculation system," *International Journal of Hydrogen Energy*, vol. 46, no. 76, pp. 38026–38039, 2021.

[77] J. Han, J. Feng, T. Hou, and X. Peng, "Performance investigation of a multi-nozzle ejector for proton exchange membrane fuel cell system," *International Journal of Energy Research*, vol. 45, no. 2, pp. 3031–3048, 2021.

[78] X. Wang, L. Wang, Y. Song, J. Deng, and Y. Zhan, "Optimal design of two-stage ejector for subzero refrigeration system on fishing vessel," *Applied Thermal Engineering*, vol. 187, article 116565, 2021.

[79] J. Han, J. Feng, T. Hou, W. Chen, and X. Peng, "Numerical and experimental study on gas-water separators for a PEMFC system," *International Journal of Green Energy*, vol. 18, no. 5, pp. 490–502, 2021.

[80] T. Ma, Y. Yang, W. Lin, Y. Yang, W. Jia, and J. Zhang, "Design of a novel high-efficiency water separator for proton exchange membrane fuel cell system," *International Journal of Hydrogen Energy*, vol. 44, no. 11, pp. 5462–5469, 2019.

[81] K. Nikiforow, H. Karimäki, T. M. Keränen, and J. Ihonen, "Optimization study of purge cycle in proton exchange membrane fuel cell system," *Journal of Power Sources*, vol. 238, pp. 336–344, 2013.

[82] X. Wang, Y. Lu, B. Zhang, J. Liu, and S. Xu, "Experimental analysis of an ejector for anode recirculation in a 10 kW polymer electrolyte membrane fuel cell system," *International Journal of Hydrogen Energy*, vol. 47, no. 3, pp. 1925–1939, 2022.

[83] J. Han, B. Zhao, Z. Pang, J. Feng, and X. Peng, "Transient characteristics investigation of the integrated ejector-driven hydrogen recirculation by multi-component CFD simulation," *International Journal of Hydrogen Energy*, vol. 47, no. 67, pp. 29053–29068, 2022.

[84] J. T. Pukrushpan, A. G. Stefanopoulou, and H. Peng, *Control of Fuel Cell Power Systems: Principles, Modeling, Analysis and Feedback Design*, Springer Science & Business Media, 2004.

[85] S. T. Thompson, B. D. James, J. M. Huya-Kouadio et al., "Direct hydrogen fuel cell electric vehicle cost analysis: system and high-volume manufacturing description, validation, and outlook," *Journal of Power Sources*, vol. 399, pp. 304–313, 2018.

[86] G. Singer, G. Gappmayer, M. Macherhammer, P. Pertl, and A. Trattner, "A development toolchain for a pulsed injector-ejector unit for PEM fuel cell applications," *International Journal of Hydrogen Energy*, vol. 47, no. 56, pp. 23818–23832, 2022.

[87] J. Zhao, X. Li, C. Shum, and J. McPhee, "Control-oriented computational fuel cell dynamics modeling–model order reduction vs. computational speed," *Energy*, vol. 266, article 126488, 2023.

[88] T. Wang, H. Huang, X. Li, X. Guo, M. Liu, and H. Lei, "Optimal estimation of proton exchange membrane fuel cell model parameters based on an improved chicken swarm optimization algorithm," *International Journal of Green Energy*, vol. 20, no. 9, pp. 946–965, 2023.

[89] B. Qin, X. Wang, L. Wang, H. Zhao, X. Yin, and L. Jia, "Hydrogen excess ratio control of ejector-based hydrogen recirculation PEM fuel cell system," in *2019 34rd Youth Academic Annual Conference of Chinese Association of Automation (YAC)*, pp. 648–653, Jinzhou, China, 2019.

[90] X. Ye, T. Zhang, H. Chen, J. Cao, and J. Chen, "Fuzzy control of hydrogen pressure in fuel cell system," *International Journal of Hydrogen Energy*, vol. 44, no. 16, pp. 8460–8466, 2019.

[91] K. Sankar and A. K. Jana, "Nonlinear multivariable sliding mode control of a reversible PEM fuel cell integrated system," *Energy Conversion and Management*, vol. 171, pp. 541–565, 2018.

[92] X. Yin, X. Wang, L. Wang et al., "Cooperative control of air and fuel feeding for PEM fuel cell with ejector-driven recirculation," *Applied Thermal Engineering*, vol. 199, article 117590, 2021.